

## Modes of Rotational Motion of Wormlike Chains and the Effect of Charges on Electrooptical Transients

Jan Antosiewicz,<sup>†</sup> Gerhard Nolte, and Dietmar Porschke\*

Max Planck Institut für Biophysikalische Chemie, 3400 Göttingen, Germany

Received March 16, 1992; Revised Manuscript Received August 10, 1992

**ABSTRACT:** Electrooptical decay curves have been calculated for ensembles of wormlike chains by averaging decay curves of individual chains generated by a Monte Carlo simulation. This procedure is valid for the limit case of very low internal mobility relative to overall rotational diffusion. Although the ensembles consist of broad distributions of chain configurations, the decay curves can be fitted by two time constants with surprisingly high accuracy. For a set of data simulated with a persistence length  $p = 450$  Å in the range of contour lengths from  $0.25p$  to  $3.64p$ , the time constants associated with the slow process lead to an apparent persistence length of 738 Å. For the case of polymers with a high charge density like DNA, the electric moments arising from nonsymmetric charge distributions may lead to electrooptical decay curves with amplitude inversion and to discontinuities in the chain length dependence of the time constants. This effect is observed for models of DNA double helices in the range of chain lengths from 100 to 250 base pairs, when the polarizability decreases from values characteristic of low salt conditions ( $\sim 1$  mM) to values found at intermediate salt concentrations ( $\sim 10$  mM). Amplitudes of electrooptical decay curves can be more useful for the assignment of these unusual effects than time constants. General predictions derived from these calculations are in agreement with experimental observations.

### Introduction

The motions of flexible polymer chains have been described by various models using approximations on different levels. Due to the complexity of potential mechanisms of coupling between the modes of motion, until now it has neither been possible to develop a comprehensive model nor to characterize the modes of motion in sufficient detail by pertinent experiments. However, more information on the relation between molecular parameters of polymer chains and the quantities observed by particular experimental techniques can be obtained by appropriate computations.

Among the available experimental techniques, measurements reflecting rotational motions provide the most sensitive information on the state of polymer chains because of the strong dependence of the rotational diffusion coefficients on the effective dimensions. However, the results are strongly influenced by internal motions of the polymer chains. Usually, this influence is considered in current theories<sup>1-3</sup> by evaluations based on simple averages. Hagerman and Zimm,<sup>3</sup> for example, used the average of diffusion coefficients calculated for randomly generated polymer chains. This procedure is an approximation for the case, where internal motions are fast relative to overall rotational diffusion. For comparison we have used a different procedure: we have calculated electrooptical decay curves for individual members of large ensembles of polymer chains separately and evaluated their sum in complete analogy to experimental data by standard exponential fitting routines. Our procedure provides a correct description for the case, where internal motions are very slow compared to overall rotational diffusion. As should be expected, the apparent overall diffusion time constants obtained by the second procedure are larger than those derived by the first one. Our computations show that even for very broad distributions of "frozen" polymer chains, the sum can be represented by two exponentials with high accuracy. This part of our simulations is complementary to part of the simulations by

Allison and Nambi,<sup>4</sup> published after completion of the first version of the present article. Some information on the rotational and internal dynamics of polymer chains has also been obtained by Lewis et al.<sup>5</sup> and very recently by Chirico and Langowski<sup>6</sup> using the Brownian dynamics approach. We have used our Monte Carlo procedure to simulate data for a wide range of chain lengths as a basis for further calculations on the effect of charges attached on the polymer chains. We show that the electrooptical decay curves and the chain length dependence of the time constants may be strongly affected by these charges. Relative amplitudes obtained from the decay curves can be more sensitive indicators for the state of the chains than the time constants.

### Simulation Procedure

Wormlike chains were generated as reported by Hagerman and Zimm<sup>3</sup> (cf. also Porschke and Nolte<sup>7</sup>). We used overlapping beads with a standard bead radius of 12.5 Å and a distance between subsequent bead centers corresponding to this bead radius. The diffusion coefficients of the individual bead assemblies were compared by the procedures discussed by Garcia de la Torre and Bloomfield<sup>8</sup> together with the volume correction described by Antosiewicz and Porschke.<sup>9</sup> All the data presented below were calculated for 20 °C with a viscosity of  $1.002 \times 10^{-3}$  kg m<sup>-1</sup> s<sup>-1</sup> corresponding to dilute aqueous solutions. The dichroism decay curves were calculated by the procedure reported by Wegener et al.<sup>10</sup> using the following parameters: the diagonal components of the local transition dipole tensor were 9100, 9100, and 1300 (corresponding to an extinction coefficient of 6500 M<sup>-1</sup> cm<sup>-1</sup> and a limit value of the reduced linear dichroism of  $-1.2$  for straight chains); the polarizabilities were calculated assuming a quadratic increase with the chain length for straight fragments according to  $p_N = N^2 f$ ; for low salt conditions we used  $f = 7.496 \times 10^{-37}$  (C m<sup>2</sup> V<sup>-1</sup>), for high salt we used  $f = 5.965 \times 10^{-38}$  (C m<sup>2</sup> V<sup>-1</sup>) (Porschke, to be published). The polarizability tensor of curved fragments was calculated by simple addition of local contributions according to the procedure described by Antosiewicz and Porschke.<sup>11</sup> Permanent dipole moments of asymmetric structures with net charges were referred to the center of diffusion, which corresponds to the center of the coordinate system, where the translational-rotational diffusion coupling tensor is symmetric. The center of diffusion was evaluated for our bead models by the procedures discussed by Harvey and Garcia de la Torre<sup>12</sup> (for details of the dipole calculation cf. ref 11). Exponential time constants were evaluated by the fitting algorithm "DISCRETE" developed by

<sup>†</sup> Permanent address: Department of Biophysics, Warsaw University, 02-089 Warsaw, Poland.

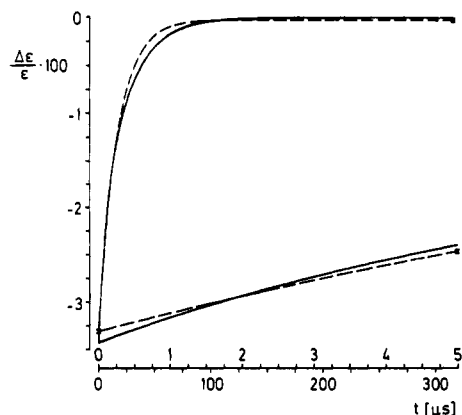


**Figure 1.** Dichroism decay curve averaged from the individual decay curves of 10 000 randomly generated chains with 120 beads, corresponding to a DNA chain length of 445 base pairs, at two time scales. The dashed line corresponds to a least squares fit by a single exponential; the simulated data and the least squares fit with two exponentials cannot be distinguished on the scale of this figure ( $\tau_1 = 5.37 \mu\text{s}$ ,  $\tau_2 = 24.0 \mu\text{s}$ ,  $A_1 = 24.0 \mu\text{s}$ ,  $A_1 = -0.0092$ ,  $A_2 = -0.0250$ ; polarizability term corresponding to low salt conditions; without consideration of dipole moments due to phosphate charges).

Provencher.<sup>13</sup> We have used DISCRETE because this or corresponding procedures have been applied previously for the evaluation of our experimental data. For comparison we have used also "CONTIN", a procedure developed by Provencher<sup>14,15</sup> for fitting of continuous distributions of relaxation time constants. However, CONTIN has not been applied as a standard for all evaluations, because it is more difficult to use than DISCRETE, when the exponentials may have both positive and negative amplitudes (cf. ref 14 and Provencher, personal communication). The amplitudes of the dichroism decay curves given below represent values of the reduced linear dichroism and are calculated under the approximation of the Kerr formalism (cf. Wegener et al.<sup>10</sup>) using an electric field strength of  $10 \text{ kV cm}^{-1}$ .

## Results

Because large fluctuations must be expected in the hydrodynamic dimensions of wormlike chains, we have generated ensembles containing at least 10 000 individual chains. An example of a dichroism decay curve obtained for an ensemble with 10 000 chains, each of them with 120 beads corresponding to a DNA chain length of 445 base pairs, is given in Figure 1. The decay curve can be represented by two exponentials at a high accuracy. Fits with two exponentials were of surprisingly high quality also for all the other simulated decay curves, although these curves represent a large variety of different chain configurations with widely different hydrodynamic dimensions. At the given accuracy of the calculated decay curves it would be possible to fit more exponentials. However, experimental data obtained for comparable systems would show at least some noise and, thus, fits with more than two exponentials would not provide reliable results.

The unexpectedly high quality of two-exponential fits may be explained by various factors. First of all, configurations with extreme hydrodynamic dimensions certainly exist but apparently do not contribute very much to the population. In addition, compact configurations contribute less than extended ones to the optical signal because of their low electrical/optical anisotropies. Finally, it is well-known that the exact evaluation of the components of exponential curves is very difficult, unless the exponentials are well separated on the time scale. In the present case, our results demonstrate that the distribution of exponentials is relatively narrow.

We have also fitted our decay curves by continuous distributions of relaxation time constants using CONTIN.<sup>13,14</sup> Decay curves simulated for chains with 130 beads could be represented by two separate distributions at high accuracy; in this case the time constants associated with maximal amplitudes are in close agreement with the time constants found by the analysis in terms of discrete exponentials. When the resolution was increased, CONTIN found an increasing number of distributions, which is due to the facts (1) that there is virtually continuous distribution of time constants and (2) that the simulated data are without noise. In analogy to the increasing accuracy of fits resulting from an increasing number of discrete exponentials, the accuracy also increases when the number of distributions of time constants is increased. Some limit has to be set under these conditions. As shown in Figure 1, the accuracy is quite satisfactory already, when the data are fitted by two discrete exponentials. Furthermore, CONTIN is more difficult to use than procedures with discrete exponentials, when amplitudes of both positive and negative sign are required (cf. below). This is a known problem (cf. ref 14 and Provencher, personal communication). Finally, a strong argument for using discrete time constants is the fact that our experimental data (and most experimental data in the literature) have also been described by discrete time constants.

Dichroism decay curves have been generated for a wide range of chain lengths with 8–130 beads corresponding to DNA double helices with 33 to 482 base pairs. For chains with more than 16 beads, the decay curves were fitted by two exponentials; for chains with 8, 12, and 16 beads single exponential fits were of sufficient quality. The time constants of the slow processes are taken as representative of the overall rotational diffusion of the chains and are interpreted by a model used for the evaluation of corresponding experimental data. We use a "combined model"<sup>16</sup> with the rotational diffusion coefficients for rigid rods given by Tirado and Garcia de la Torre<sup>17,18</sup> together with correction factors for wormlike chain flexibility derived from Monte Carlo simulations by Hagerman and Zimm.<sup>3</sup> By this procedure we get for decay curves simulated with an "input" persistence length of 450 Å an "output" persistence length of 738 Å (cf. Figure 2). Thus, as should be expected, the apparent persistence length for a system with frozen internal mobility is clearly larger than the "input" persistence length. For comparison we have also used the procedure applied by Hagerman and Zimm<sup>3</sup> for the case of fast equilibration of internal modes with direct averaging of the coefficients for overall rotational diffusion: from the ensemble of chains used for the evaluation described above we get a persistence length of 458 Å, which is in very satisfactory agreement with the "input" persistence length.

For the simulations described above, the electrooptical effect was induced due to the polarizability, which was included in the alignment tensor. However, electrooptical effects of nucleic acids may also be induced by an asymmetrical distribution of phosphate charges, which may lead to large "permanent" dipole moments.<sup>11</sup> Most of the configurations of wormlike chains are asymmetric, and thus, their alignment may partially be caused by contributions due to a permanent dipole moment. The magnitude of the permanent dipole is, of course, strongly dependent on the effective charge of phosphate residues, which is not exactly known. We have simulated dichroism decay curves for a charge density corresponding to that of DNA double helices with uniform effective phosphate charges corresponding to 15% of the elementary charge

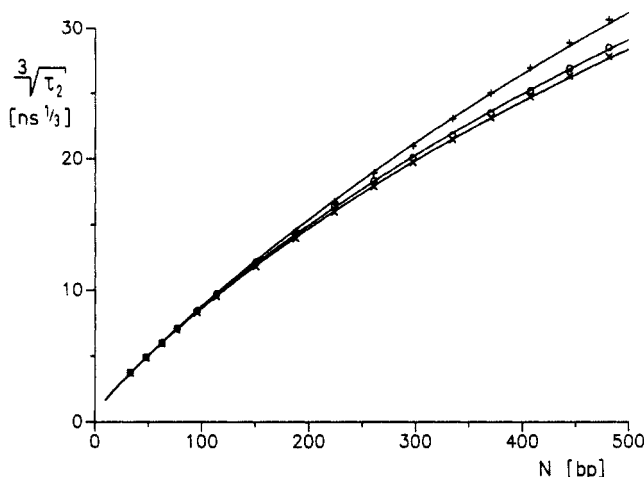


**Figure 2.** Third root of the second time constant  $\tau_2^{1/3}$  in  $\text{ns}^{1/3}$  as a function of the chain length  $N$  in base pairs from fits of averaged dichroism decay curves calculated (a) without consideration of dipole moments from phosphate charges (+) and (b) with low salt polarizability and phosphate charges corresponding to  $0.15e$  (O). Time constants calculated from averaged diffusion coefficients representing overall rotational diffusion (X) are shown for comparison. The continuous lines represent least squares fits by the combined model with the following fit parameters: persistence length  $p = 738 \text{ \AA}$ , radius  $r = 10.2 \text{ \AA}$  (+);  $p = 504 \text{ \AA}$ ,  $r = 11.2 \text{ \AA}$  (O);  $p = 458 \text{ \AA}$ ,  $r = 10.8 \text{ \AA}$  (X).

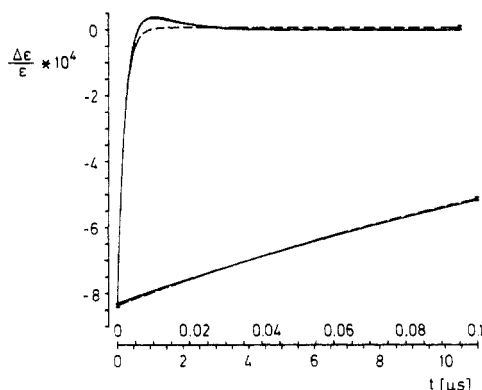


**Figure 3.** Dichroism decay curve averaged from the individual decay curves of 20 000 randomly generated chains with 35 beads, corresponding to a DNA chain length of 132 base pairs at two time scales. The dashed line corresponds to a least squares fit by a single exponential; the simulated data and the least squares fit with two exponentials cannot be distinguished on the scale of this figure ( $\tau_1 = 0.238 \text{ \mu s}$ ,  $\tau_2 = 1.176 \text{ \mu s}$ ,  $A_1 = -9.43 \times 10^{-4}$ ,  $A_2 = 1.15 \times 10^{-3}$ ; polarizability term corresponding to high salt conditions; with consideration of the dipole moment due to phosphate charges corresponding to 15% of the elementary charge).

(cf. reviews of polyelectrolyte theory<sup>19,20</sup>). Again the curves could be fitted by two exponentials at a satisfactory accuracy and the time constants corresponding to the slow component were fitted by the combined model:<sup>16</sup> in this case the persistence length is  $504 \text{ \AA}$ .

For the simulations described above we used polarizabilities, which have been observed under low salt conditions in the range 1–2 mM monovalent salt concentration. At higher salt concentrations the polarizability decreases and, thus, the influence of the permanent dipole contribution should increase. We have simulated the transient dichroism with polarizabilities, which are close to those observed at 12 mM monovalent salt concentration, and found decay curves with very special inversion shapes (cf. Figure 3). Dichroism decay curves with inversion of amplitudes have been calculated previously for curved DNA fragments and have been observed for DNA double

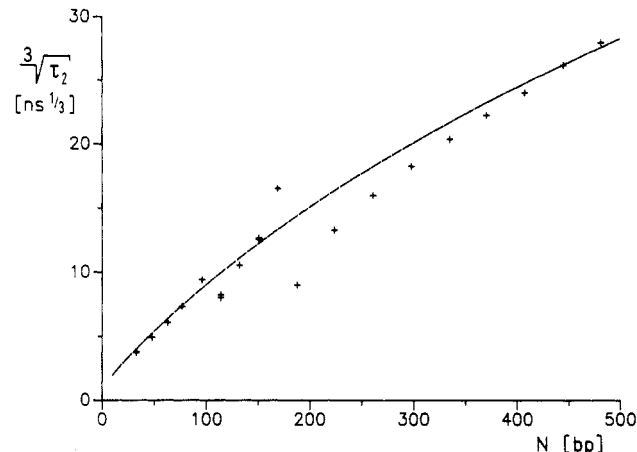


**Figure 4.** Third root of the second time constant  $\tau_2^{1/3}$  in  $\text{ns}^{1/3}$  as a function of the chain length  $N$  in base pairs from fits of averaged dichroism decay curves calculated with the high salt polarizability and phosphate charges corresponding to  $0.15e$ . The continuous line represents a least squares fit by the "combined" model with a persistence length  $p = 397 \text{ \AA}$  and a radius  $r = 15.6 \text{ \AA}$ .

helices in a range of chain lengths around 180 bp at high salt concentrations of 12 mM (cf. ref 11). Because the great majority of the configurations generated by the Monte Carlo procedure are curved, the unusual electrooptical effect is found again. In close analogy with the experimental observations, the curves with amplitude inversion are found in our simulation only in the same restricted range of chain lengths.

The special effects resulting from the contribution of the permanent dipole moment are reflected by a very peculiar dependence of the time constants on the chain length. As shown in Figure 4, the time constants do not increase continuously with the chain length. Apparently, the discontinuities result from acceleration and retardation effects of the dichroism decay,<sup>11</sup> which are not due to changes of the diffusion coefficients but are caused by large changes in the amplitudes of the five processes associated with the dichroism decay of particles without symmetry.<sup>10</sup>

For the calculations described above we have used a constant effective phosphate charge corresponding to 15% of the elementary charge. For comparison we have also calculated a set of data with an effective phosphate charge corresponding to 10% of the elementary charge together with the high salt polarizability. As shown in Figure 5, the dependence of the time constants on the chain length is smoothed out upon reduction of the phosphate charge. Nevertheless, the influence of the permanent dipole moment remains detectable by a distorted dependence of the time constant on the chain length. Due to the distortion, the simulated data cannot be represented by our standard model for the rotational time constants of wormlike chains with the usual accuracy.

A very useful but often neglected source of information is the amplitudes associated with individual relaxation effects. A comparison of the relative amplitudes  $A_1$  associated with the fast process of the dichroism decay curves (cf. Figure 6) reveals a difference for two sets of data, which is much larger than expected. The  $A_1$  values found for the case with the phosphate charge  $0.15e$  and the low salt polarizability increase much more strongly with the chain length than those found for the same polarizability at zero phosphate charge. As described above, the time constants for these two cases are different, but not as much as the amplitudes  $A_1$ . Thus, the

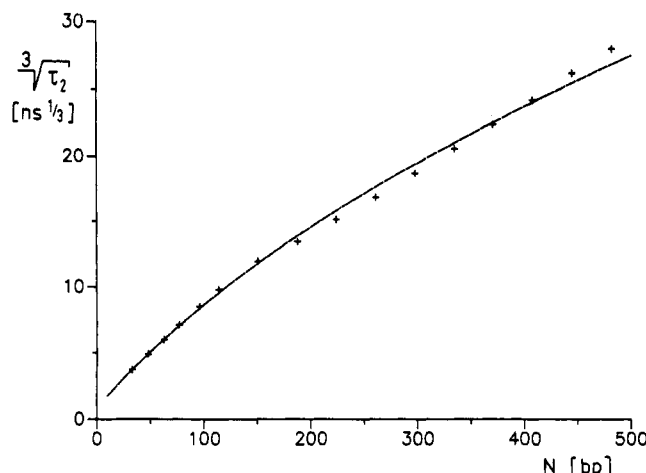


**Figure 5.** Third root of the second time constant  $\tau_2^{1/3}$  in  $\text{ns}^{1/3}$  as a function of the chain length  $N$  in base pairs from fits of averaged dichroism decay curves calculated with the high salt polarizability and phosphate charges corresponding to  $0.10e$ . The continuous lines represent least squares fits by the combined model with a persistence length  $p = 394 \text{ \AA}$  and a radius  $r = 11.8 \text{ \AA}$ .

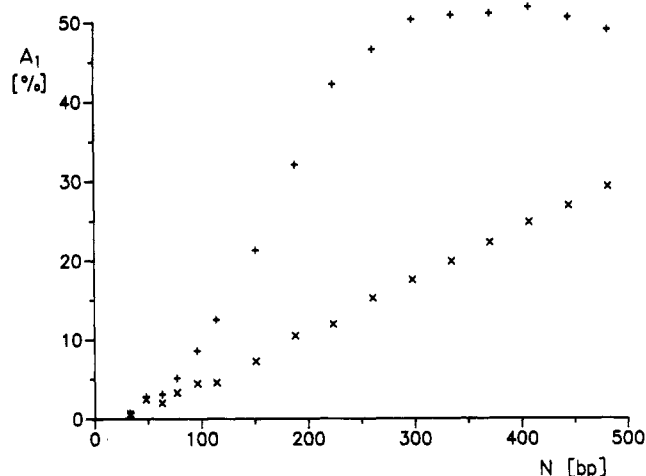


**Figure 6.** Amplitude  $A_1$  associated with the fast dichroism decay process relative to the total amplitude in percent as a function of the chain length  $N$  given in base pairs (calculated with the low salt polarizability term; permanent dipole moments due to phosphate charges corresponding to 15% of the elementary charge included (+) and not included (x)).

amplitudes may be more useful to distinguish between different cases than the time constants.

The amplitudes  $A_1$  are calculated in the present simulations without consideration of field-induced changes of the polymer configuration and, thus, should correspond to experimental values extrapolated to zero electric field strength. Experiments performed on a DNA restriction fragment with 179 base pairs indicate that the corresponding amplitude is in the range below 10% at low salt concentrations.<sup>21</sup> According to this result the effective phosphate charge is below  $0.15e$  at the low salt concentration (cf. Figure 6). The bending amplitudes analyzed in previous communications<sup>21,22</sup> result from field-induced stretching of DNA double helices and do not correspond to the amplitudes  $A_1$  discussed above.

Finally, the magnitude of the time constants  $\tau_1$  associated with the fast part of the decay process should at least be mentioned: in the case of the low salt polarizability without consideration of the permanent dipole effect due to phosphate charges, the  $\tau_1$  values are in the range 20–30% of the time constants  $\tau_2$ . Experimental time constants found for the fast process in the dichroism decay of DNA

double helices after high electric field pulses have been assigned to bending and are at 7–9% of the time constants associated with overall rotation.<sup>16</sup> This is again evidence for the interpretation that the bending process assigned previously and the fast process found in our present simulations are not equivalent.

## Discussion

The structure and dynamics of large wormlike molecules in general and of DNA in particular have been analyzed by various experimental and theoretical procedures. Among the experimental techniques, electrooptical ones<sup>23,24</sup> have been particularly useful because of their high sensitivity. Time constants obtained by recent measurements have been interpreted preferentially by the model of Hagerman and Zimm,<sup>3</sup> which is based on the assumption of fast equilibration of internal modes. It is not clear, however, whether this assumption is valid for all cases and/or under all experimental conditions.

Our present simulations for the case of frozen internal dynamics provide several results. First of all, it is shown that a broad distribution of configurations does not lead to a particularly broad distribution of time constants. Thus, the experimental observation of a narrow distribution of time constants does not prove high internal dynamics of the system under investigation. As expected, the time constants for the case of frozen internal modes are larger than those for the case with high internal mobility.

This part of our simulations is closely related to simulations by Allison and Nambi. These authors used for part of their calculations a model very similar to our frozen ensemble model, but also simulated the Brownian dynamics of flexible chains. They conclude that “rigid” ensemble models are able to account reasonably well for the longest relaxation time”. A comparison shows that the time constants resulting from the Hagerman/Zimm procedure are indeed rather close to the ones obtained by Brownian dynamics for flexible chains. However, our time constants for frozen ensembles are clearly larger than those for flexible chains (e.g. by 34% at a contour length of 482 base pairs). The difference may be partly due to details in the evaluation of the data. The parameters obtained from fitting of multiexponential decay curves are strongly dependent on “weighing” of the data points, which often occurs unconsciously, e.g. by the selection of the time range of the input data. Processing of our simulated data, as documented by the example given in Figure 1, has been as close as possible to that used for our experimental data. Some difference may also be due to details of the orientation mechanism.

Our simulations provide a particularly striking example for the strong influence of the orientation mechanism and demonstrate the potential effect of nonsymmetric distributions of charges. An exact quantitative description of this effect is difficult for various reasons. The effective charge associated with polyelectrolyte residues can hardly be assigned with sufficient accuracy. The values used for our calculations are estimated according to the current state of polyelectrolyte theory.<sup>19,20</sup> We have used constant values of the effective charge along the polymer chains, although it may be expected that this parameter is not identical at the center and at the ends of the chains. Moreover, shielding of these charges by ions in the solutions requires a more detailed description than using a simple reduced effective charge. Finally, we have used a rather simple model for our calculation of the polarizability tensor and did not account for changes in the ion distribution resulting from the external electric field. In view of these

approximations, it is remarkable that the predictions derived from our model are at least in qualitative agreement with the available experimental results. The dichroism decay curves with amplitude inversion have been observed<sup>11</sup> in the range predicted by the model. Thus, the major factors contributing to the unusual effects have been assigned correctly.

The experiments indicate that the unusual dichroism effects are at least partly induced by electric field pulses with a time constant in the microsecond time range. According to these observations the special dipole moment causing the unusual dichroism effects may be amplified by electric field pulses. Two different mechanisms may contribute: the electric field may increase DNA bending and/or the electric field may induce biased dissociation of ions. The coupling of all these effects during application of electric field pulses remains a challenge for a future quantitative description. From the present simulations we have learned that the unusual dichroism effects must be expected already for standard distributions of charged wormlike chains without contributions by field-induced reactions. More detailed assignments of various contributions are possible by Brownian dynamic simulations, for example. However, such simulations require much more computer time.

**Acknowledgment.** For our computations we used the facilities of the Gesellschaft für wissenschaftliche Datenverarbeitung m.b.H., Göttingen.

## References and Notes

- (1) Hearst, J. J. *J. Chem. Phys.* **1963**, *38*, 1062.
- (2) Yamakawa, H.; Yamaki, J. *J. Chem. Phys.* **1973**, *58*, 2049.
- (3) Hagerman, P. J.; Zimm, B. H. *Biopolymers* **1981**, *20*, 1481.
- (4) Allison, S. A.; Nambi, P. *Macromolecules* **1992**, *25*, 759.
- (5) Lewis, R. J.; Allison, S. A.; Eden, D.; Pecora, R. *J. Chem. Phys.* **1988**, *89*, 2490.
- (6) Chirico, G.; Langowski, J. *Macromolecules* **1992**, *25*, 769.
- (7) Porschke, D.; Nolte, G. *Biopolymers* **1990**, *30*, 1289.
- (8) Garcia de la Torre, J.; Bloomfield, V. A. *Quart. Rev. Biophys.* **1981**, *14*, 81.
- (9) Antosiewicz, J.; Porschke, D. *J. Phys. Chem.* **1989**, *93*, 5301.
- (10) Wegener, W. A.; Dowben, R. M.; Koester, V. J. *J. Chem. Phys.* **1979**, *70*, 622.
- (11) Antosiewicz, J.; Porschke, D. *Biophys. Chem.* **1989**, *33*, 19.
- (12) Harvey, S. C.; Garcia de la Torre, J. *Macromolecules* **1980**, *13*, 960.
- (13) Provencher, S. W. *Biophys. J.* **1976**, *16*, 27.
- (14) Provencher, S. W. *Comput. Phys. Commun.* **1982**, *27*, 213.
- (15) Provencher, S. W. *Comput. Phys. Commun.* **1982**, *27*, 229.
- (16) Porschke, D. *Biophys. Chem.* **1991**, *40*, 169.
- (17) Tirado, M. M.; Garcia de la Torre, J. *J. Chem. Phys.* **1980**, *73*, 1986.
- (18) Tirado, M. M.; Martinez, C. L.; Garcia de la Torre, J. *J. Chem. Phys.* **1984**, *81*, 2047.
- (19) Manning, G. S. *Quart. Rev. Biophys.* **1978**, *11*, 179.
- (20) Record, M. T.; Anderson, C. F.; Lohman, T. M. *Quart. Rev. Biophys.* **1978**, *11*, 103.
- (21) Porschke, D. *J. Biomol. Struct. Dyn.* **1986**, *3*, 373.
- (22) Porschke, D. *Biopolymers* **1989**, *28*, 1383.
- (23) Fredericq, E.; Houssier, C. *Electric Dichroism and Electric Birefringence*; Clarendon: Oxford, U.K., 1973.
- (24) O'Konski, C. T. *Molecular Electrooptics, I Theory and Methods, II Applications to Biopolymers*; Dekker: New York, 1976, 1978.